

# Galactic Point Sources of TeV Antineutrinos

Luis A. Anchordoqui<sup>a</sup>, Haim Goldberg<sup>a</sup>, Francis Halzen<sup>b</sup>, and Thomas J. Weiler<sup>b,c,d</sup>

<sup>a</sup>*Department of Physics, Northeastern University, Boston MA 02155*

<sup>b</sup>*Department of Physics, University of Wisconsin, Madison WI 53706*

<sup>c</sup>*Center for Cosmological Physics, University of Chicago, Chicago IL 60637*

<sup>d</sup>*Department of Physics and Astronomy, Vanderbilt University, Nashville TN 37235*

High energy cosmic ray experiments have identified an excess from the region of the Galactic Plane in a limited energy range around  $10^{18}$  eV (EeV). This is very suggestive of neutrons as candidate primaries, because the directional signal requires relatively-stable neutral primaries, and time-dilated neutrons can reach Earth from typical Galactic distances when the neutron energy exceeds an EeV. We here point out that if the Galactic messengers are neutrons, then those with energies below an EeV will decay in flight, providing a flux of cosmic antineutrinos above a TeV which is *observable* at a kilometer-scale neutrino observatory. The expected event rate per year above 1 TeV in a detector such as IceCube, for example, is 20 antineutrino showers (all flavors) and a  $1^\circ$  directional signal of 4  $\bar{\nu}_\mu$  events. A measurement of this flux can serve to identify the first extraterrestrial point source of TeV antineutrinos.

PACS numbers: 13.85.Tp, 95.85.Ry, 95.30.Cq

An intriguing anisotropy in the cosmic ray spectrum has emerged in the energy range near an EeV. The Akeno Giant Air Shower Array (AGASA) has revealed a correlation of the arrival direction of the cosmic rays to the Galactic Plane (GP) at the  $4\sigma$  level [1]. The GP excess, which is roughly 4% of the diffuse flux, is mostly concentrated in the direction of the Cygnus region, with a second spot towards the Galactic Center (GC) [2]. Evidence at the  $3.2\sigma$  level for GP enhancement in a similar energy range has also been reported by the Fly's Eye Collaboration [3]. The existence of a point-like excess in the direction of the GC has been confirmed via independent analysis [4] of data collected with the Sydney University Giant Airshower Recorder (SUGAR). This is a remarkable level of agreement among experiment using a variety of techniques.

Independent evidence may be emerging for a cosmic accelerator in the Cygnus spiral arm. The HEGRA experiment has detected an extended TeV  $\gamma$ -ray source in the Cygnus region with no clear counterpart and a spectrum not easily accommodated with synchrotron radiation by electrons [5]. The difficulty to accommodate the spectrum by conventional electromagnetic mechanisms has been exacerbated by the failure of CHANDRA and VLA to detect X-rays or radiowaves signaling acceleration of any electrons [6]. The model proposed is that of a proton beam, accelerated by a nearby mini-quasar or possibly Cygnus X-3, interacting with a molecular cloud to produce pions that are the source of the gamma rays. Especially intriguing is the possible association of this source with Cygnus-OB2, a cluster of more than 2700 (identified) young, hot stars with a total mass of  $\sim 10^4$  solar masses [7]. Proton acceleration to explain the TeV photon signal requires only 0.1% efficiency for the conversion of the energy in the stellar wind into cosmic ray acceleration. Also, the stars in Cygnus-OB2 could be the

origin of time-correlated, clustered supernova remnants forming a source of cosmic rays. By cooperative acceleration their energies may even exceed the  $\sim 1$  PeV cutoff of individual remnants and accommodate cosmic rays up to the ankle, where the steeply falling ( $\propto E^{-3.16 \pm 0.08}$ ) cosmic ray spectrum flattens to  $E^{-2.8 \pm 0.3}$  [8].

All evidence points to a transition from galactic to extragalactic sources above several EeV of primary energy. The steepness of the falloff between the knee (about 3 PeV) and the ankle (about 10 EeV) is expected from supernova shock models, and may indicate that we are witnessing the high energy end of the galactic flux. The extension of the nominal PeV cutoff beyond the ankle can be understood as a collective effect of stellar winds originating in the region of multiple supernova explosions. These provide a second acceleration to the particles and boost their energies far beyond the values expected from their single-shock encounter. Strong additional support for this picture emerges from accumulating evidence (in a bi-modal proton-iron model) for a dominant Fe component in the flux [9]. The importance of the heavy component is apparent all the way down to the region of several PeV [10], with the spectral index hardening slightly to  $3.02 \pm 0.03$  below 500 PeV. *An immediate consequence of this nucleus-dominance picture is the creation of free neutrons via nuclei photodisintegration on background photon fields.* These liberated neutrons are presumably responsible for the observed directional signals. *This implies that it may not be a coincidence that the signal appears first at energies where the neutron lifetime allows propagation distances of galactic scales, i.e., 10 kpc.*

For every surviving neutron at  $\sim$  EeV, there are many neutrons at lower energy that decay via  $n \rightarrow p + e^- + \bar{\nu}_e$ . The decay mfp of a neutron is  $c\Gamma_n \bar{\tau}_n = 10 (E_n/\text{EeV})$  kpc, the lifetime being boosted from its rest-frame value  $\bar{\tau}_n = 886$  seconds to its lab value via

$\Gamma_n = E_n/m_n$ . The proton is bent by the Galactic magnetic field, the electron quickly loses energy via synchrotron radiation, and the  $\bar{\nu}_e$  travels along the initial neutron direction, producing a directed TeV energy beam whose flux is calculable. *We show in this Letter that the expected  $\bar{\nu}$  flux from the direction of the Cygnus region is measurable in IceCube [11].* Furthermore, by the same logic, a km-scale Mediterranean detector, if designed with sufficiently low threshold, can see the  $\bar{\nu}$

flux pointing toward the GC source as well. The GZK neutrinos [12] and the “essentially guaranteed”  $\bar{\nu}$  flux calculated here probably constitute the best motivated cosmic neutrino fluxes. Of these two neutrino fluxes, the expected event rate for the galactic beam is higher: 4  $\bar{\nu}_\mu$  events per year and 16 in  $\bar{\nu}_e + \bar{\nu}_\tau$  showers.

We turn to the calculation. The basic formula that relates the neutron flux at the source ( $dF_n/dE_n$ ) to the antineutrino flux observed at Earth ( $dF_{\bar{\nu}}/dE_{\bar{\nu}}$ ) is:

$$\frac{dF_{\bar{\nu}}}{dE_{\bar{\nu}}}(E_{\bar{\nu}}) = \int dE_n \frac{dF_n}{dE_n}(E_n) \left(1 - e^{-\frac{D m_n}{E_n \bar{\tau}_n}}\right) \int_0^Q d\epsilon_{\bar{\nu}} \frac{dP}{d\epsilon_{\bar{\nu}}}(\epsilon_{\bar{\nu}}) \int_{-1}^1 \frac{d \cos \bar{\theta}_{\bar{\nu}}}{2} \delta[E_{\bar{\nu}} - E_n \epsilon_{\bar{\nu}} (1 + \cos \bar{\theta}_{\bar{\nu}})/m_n] . \quad (1)$$

The variables appearing in Eq. (1) are the antineutrino and neutron energies in the lab ( $E_{\bar{\nu}}$  and  $E_n$ ), the antineutrino angle with respect to the direction of the neutron momentum, in the neutron rest-frame ( $\bar{\theta}_{\bar{\nu}}$ ), and the antineutrino energy in the neutron rest-frame ( $\epsilon_{\bar{\nu}}$ ). The last three variables are not observed by a laboratory neutrino-detector, and so are integrated over. The observable  $E_{\bar{\nu}}$  is held fixed. The delta-function relates the neutrino energy in the lab to the three integration variables. The parameters appearing in Eq. (1) are the neutron mass and rest-frame lifetime ( $m_n$  and  $\bar{\tau}_n$ ), and the distance to the neutron source ( $D$ ).  $dF_n/dE_n$  is the neutron flux at the source, or equivalently, the neutron flux that would be observed from the source region in the absence of neutron decay. Finally,  $\frac{dP}{d\epsilon_{\bar{\nu}}}(\epsilon_{\bar{\nu}})$  is the normalized probability that the decaying neutron in its rest-frame produces a  $\bar{\nu}_e$  with energy  $\epsilon_{\bar{\nu}}$ ;  $\int_0^Q d\epsilon_{\bar{\nu}} \frac{dP}{d\epsilon_{\bar{\nu}}}(\epsilon_{\bar{\nu}}) = 1$  defines the normalization, where the maximum neutrino energy in the neutron rest frame is just  $Q \equiv m_n - m_p - m_e = 0.71$  MeV, and the minimum neutrino energy is zero in the massless limit.<sup>1</sup> For the decay of unpolarized neutrons, there is no angular dependence in  $\frac{dP}{d\epsilon_{\bar{\nu}}}$ .

The  $E_n$  integration in Eq. (1) is effectively cut off at  $\sim$  EeV, the energy beyond which a neutron is stable over a 10 kpc path-length, and it is truly cut off by the  $E_{\max}$  of the neutron spectrum. The expression in parentheses in Eq. (1) is the decay probability for a neutron with lab energy  $E_n$ , traveling a distance  $D$ . In principle, one should consider a source distribution, and integrate over the volume  $\int d^3D$ . Instead, we will take  $D$  to be the 1.7 kpc distance from Earth to Cygnus OB2; for the purpose of generating the associated neutrino flux, this cannot be

in error by too much.

The Galactic anisotropy observed by the various collaborations spans the energy range 0.8 to 2.0 EeV.<sup>2</sup> The lower cutoff specifies that only neutrons with EeV energies and above have a boosted  $c\tau_n$  sufficiently large to serve as Galactic messengers. The upper cutoff reflects an important feature of photodisintegration at the source: heavy nuclei with energies in the vicinity of the ankle will fragment to neutrons with energies about an order of magnitude smaller. To account for the largest neutron energies, it may be necessary to populate the heavier nucleus spectrum in the region above the ankle. This is not a problem – one fully expects the emerging harder extragalactic spectrum to overtake and hide the steeply falling galactic population. It is not therefore surprising that in order to fit the spectrum in the anisotropy region and maintain continuity to the ankle region without introducing a cutoff, the AGASA Collaboration required a spectrum  $\propto E^{-3}$  or steeper [1].

A detailed scenario for ultrahigh energy nuclei (parents of the anisotropy neutrons) originating in a pulsar close to the Cygnus OB2 region has been recently described [14]. The sequence begins with the one-shot acceleration in the spinning neutron star [15], resulting in an  $E^{-1}$  spectrum. Softening of the spectrum to  $E^{-2}$  ensues through gravitational wave losses during spin-down [16]. Following this scheme, we assume that some of the nuclei are captured in the dense region of the source, attaining sufficient diffusion in milliGauss magnetic fields. The resulting time delay of several thou-

<sup>1</sup> The massless-neutrino approximation seems justifiable here: even an eV-mass neutrino produced at rest in the neutron rest-frame would have a lab energy of  $m_\nu \Gamma_n \lesssim$  GeV, below threshold for neutrino telescopes.

<sup>2</sup> Actually, the anisotropy reported in [3] peaks in the energy bin 0.4–1.0 EeV, but persists with statistical significance to energies as low as 0.2 EeV. The full Fly’s Eye data include a directional signal which was somewhat lost in unsuccessful attempts [13] to relate it to  $\gamma$ -ray emission from Cygnus X-3. This implies that if neutrons are the carriers of the anisotropy, there *needs to be* some contribution from at least one source closer than 3-4 kpc.

sand years[17] produces a further steepening of the injection power law spectrum. Note that once diffusion has been established, additional Rayleigh steps in the Galactic magnetic field do not change the spectral index significantly. In their random traversal of the OB association, the nuclei undergo photodisintegration on far infrared thermal photons populating molecular clouds with temperatures of 15-100 K [18]. Taking an average photodisintegration cross section of 40 mb, we find an interaction time between 4 and 1300 yr, allowing sufficient neutron production to explain the anisotropy.

To incorporate the preceding discussion in our work, we take in what follows a single power law neutron spectrum with a spectral index of 3.1, representing an average over the PeV-EeV energy region. Specifically,  $dF_n/dE_n = C E_n^{-3.1}$ , with the normalization constant fixed near an EeV to the observed excess. The constant  $C$  is determined by integrating  $dF_n/dE_n$  over a bin  $(E_1, E_2)$  with the result

$$F_n = \int_{E_1}^{E_2} C E_n^{-3.1} = 0.95 C \bar{E}_n^{-2.1} \sinh[1.1 \Delta], \quad (2)$$

where  $\bar{E}_n = \sqrt{E_1 E_2} \approx 10^{9.2}$  GeV,  $\Delta = \ln(E_2/E_1) \approx 1.38$ , and  $F_n \approx 9 \text{ km}^{-2} \text{ yr}^{-1}$  [2].

The typical energy for the antineutrino in the lab is that of the decaying neutron times  $Q/m_n \sim 10^{-3}$ . Thus, the stability of neutrons at  $\gtrsim$  EeV implies a PeV upper limit for the produced antineutrinos. The increasing abundance of neutrons below an EeV in turn implies an increasing neutrino flux as energies move below a PeV.

Nuclei with Lorentz factor  $\sim 10^6$  are synthesized in all supernovae. Hadronic interactions with the HII population (density  $30 \text{ cm}^{-3}$  [6]) and photodisintegration from ultraviolet photons emitted from OB stars results in a flux of PeV neutrons. From the measured Lyman emission of the O stars [7], the O+B temperature, and luminosity characteristics of the B stars [19], we obtain a photon number density in the ultraviolet of  $\sim 230 \text{ cm}^{-3}$  for the core region  $\sim 10 \text{ pc}$ . This implies a collision time of about 0.1 Myr, comparable to the time scale for hadronic interactions. However, in contrast to hadronic interactions, significant photodisintegration occurs in the outer 20 pc of the source. The photon density is reduced to  $\gtrsim 25 \text{ cm}^{-3}$ , which lengthens the reaction time to  $\sim 1 \text{ Myr}$ . The diffusion time ( $\sim 1.2 \text{ Myr}$ ) is a bit smaller than the age of the cluster  $\sim 2.5 \text{ Myr}$  [20], and somewhat higher than the reaction time. This is sufficient to permit over 90% efficiency for photodisintegration over the lifetime of the source. The effective volume for photodisintegration is then about a factor of 27 larger than for hadronic interactions, and the net result of all these considerations is that the PeV neutron population is about an order of magnitude greater than TeV charged pions resulting from hadronic collisions [21].

Performing the  $\cos\bar{\theta}_{\bar{\nu}}$ -integration in Eq. (1) over the

delta-function constraint leads to

$$\begin{aligned} \frac{dF_{\bar{\nu}}}{dE_{\bar{\nu}}}(E_{\bar{\nu}}) &= \frac{m_n}{2} \int_{E_n^{\min}} \frac{dE_n}{E_n} \frac{dF_n}{dE_n}(E_n) \left(1 - e^{-\frac{D}{E_n} \frac{m_n}{\tau_n}}\right) \\ &\times \int_{\epsilon_{\bar{\nu}}^{\min}}^Q \frac{d\epsilon_{\bar{\nu}}}{\epsilon_{\bar{\nu}}} \frac{dP}{d\epsilon_{\bar{\nu}}}(\epsilon_{\bar{\nu}}), \end{aligned} \quad (3)$$

with  $\epsilon_{\bar{\nu}}^{\min} = \frac{E_{\bar{\nu}} m_n}{2E_n}$ , and  $E_n^{\min} = \frac{E_{\bar{\nu}} m_n}{2Q}$ . An approximate answer is available. Setting the beta-decay neutrino energy  $\epsilon_{\bar{\nu}}$  equal to its mean value  $\equiv \epsilon_0$ , we have  $\frac{dP}{d\epsilon_{\bar{\nu}}}(\epsilon_{\bar{\nu}}) = \delta(\epsilon_{\bar{\nu}} - \epsilon_0)$ .<sup>3</sup> When the delta-function is substituted into Eq. (3), one gets

$$\frac{dF_{\bar{\nu}}}{dE_{\bar{\nu}}}(E_{\bar{\nu}}) = \frac{m_n}{2\epsilon_0} \int_{\frac{m_n E_{\bar{\nu}}}{2\epsilon_0}} \frac{dE_n}{E_n} \frac{dF_n}{dE_n}(E_n) \left(1 - e^{-\frac{D}{E_n} \frac{m_n}{\tau_n}}\right). \quad (4)$$

Further approximation is available. Treating the neutron decay factor,  $1 - \exp(\dots)$ , as a step function  $\Theta(E_n^{\max} - E_n)$  at some energy  $E_n^{\max} \sim \mathcal{O}(\frac{D}{\tau_n}) = (\frac{D}{10 \text{ kpc}}) \text{ EeV}$ , i.e. the neutron is unstable for  $E_n < E_n^{\max}$  and stable for  $E_n > E_n^{\max}$ , one obtains from Eq. (4)

$$\frac{dF_{\bar{\nu}}}{dE_{\bar{\nu}}}(E_{\bar{\nu}}) = \frac{m_n}{2\epsilon_0} \int_{\frac{m_n E_{\bar{\nu}}}{2\epsilon_0}}^{E_n^{\max}} \frac{dE_n}{E_n} \frac{dF_n}{dE_n}(E_n). \quad (5)$$

We have found that for  $E_n^{\max} = 3 \text{ EeV}$ , Eqs. (4) and (5) differ by less than 1% for  $E_{\bar{\nu}}$  as high as 1 PeV.

A direct  $\bar{\nu}_e$  event in IceCube will make a showering event, which, even if seen, provides little angular resolution. In the energy region below 1 PeV, IceCube will resolve directionality only for  $\nu_\mu$  and  $\bar{\nu}_\mu$ . Fortunately, neutrino oscillations rescue the signal. Since the distance to the Cygnus region greatly exceeds the  $\bar{\nu}_e$  oscillation length  $\lambda_{\text{osc}} \sim 10^{-2} \frac{E_{\bar{\nu}}}{\text{PeV}}$  parsecs (taking the solar oscillation scale  $\delta m^2 \sim 10^{-5} \text{ eV}^2$ ), the antineutrinos decohere in transit. The arriving antineutrinos are distributed over flavors, with the muon antineutrino flux  $F_{\bar{\nu}_\mu}$  given by the factor  $\frac{1}{4} \sin^2(2\theta_\odot) \simeq 0.20$  times the original  $F_{\bar{\nu}_e}$  flux. The  $\bar{\nu}_\tau$  flux is the same, and the  $\bar{\nu}_e$  flux is 0.6 times the original flux. Here we have utilized for the solar mixing angle the most recent SNO result  $\theta_\odot \simeq 32.5^\circ$  [22], along with maximal mixing for atmospheric  $\nu_\mu$ - $\nu_\tau$  neutrinos and a negligible  $\nu_e$  component in the third neutrino eigenstate.

The integral neutrino flux  $F_{\bar{\nu}}(> E_{\bar{\nu}}) \equiv \int_{E_{\bar{\nu}}} dE_{\bar{\nu}} \frac{dF_{\bar{\nu}}}{dE_{\bar{\nu}}}$  is particularly useful for experiments having a neutrino

<sup>3</sup> The delta-function in the neutron frame gives rise to a flat spectrum for the neutrino energy in the lab for fixed neutron lab-energy  $E_n = \Gamma_n m_n$ :

$$\frac{dP}{dE_{\bar{\nu}}} = \int_{-1}^1 \frac{d\cos\bar{\theta}_{\bar{\nu}}}{2} \left( \frac{d\epsilon_{\bar{\nu}}}{dE_{\bar{\nu}}} \right) \left( \frac{dP}{d\epsilon_{\bar{\nu}}} \right) = \frac{1}{2\Gamma_n \epsilon_0},$$

with  $0 \leq E_{\bar{\nu}} \leq 2\Gamma_n \epsilon_0$ .

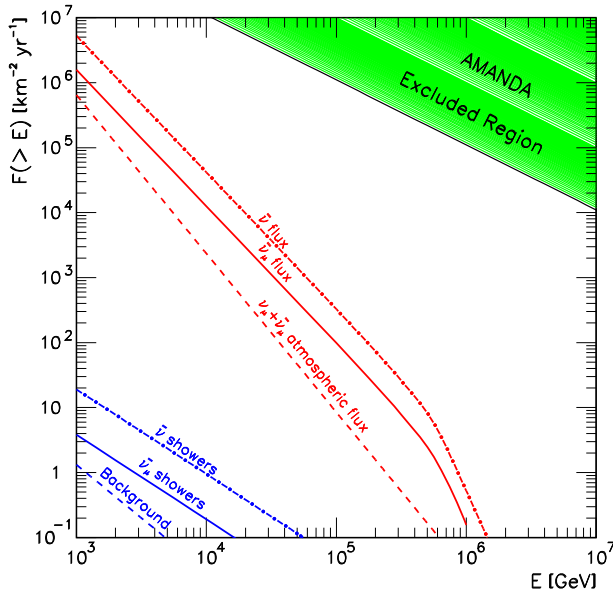


FIG. 1: Integrated flux of  $\bar{\nu}_\mu$  (solid) and  $\bar{\nu}_\mu + \bar{\nu}_e + \bar{\nu}_\tau$  (dashed-dotted) predicted to arrive at Earth from the direction of the Cygnus region. Also shown is the integrated  $\nu_\mu + \bar{\nu}_\mu$  atmospheric flux for an angular bin of  $1^\circ \times 1^\circ$ . The shaded band indicates the region excluded by the AMANDA experiment [23]. The expected number of showers  $\bar{\nu}_\mu$  (solid) and  $\bar{\nu}_\mu + \bar{\nu}_e + \bar{\nu}_\tau$  (dashed-dotted) to be detected (say in IceCube) are plotted on the bottom-left. The expected background for the same angular bin is indicated by the dashed line.

detection-efficiency that is independent of neutrino energy, or nearly so. IceCube is an example of such an experiment. Our calculated integral flux is shown in Fig. 1. As mentioned above, the nuclear photodisintegration threshold leads to an infrared cutoff on the primary neutron energy at the source, which in turn leads to a low energy cutoff  $\sim$  TeV on the integral flux.

We now estimate the signal-to-noise ratio at IceCube. The angular resolution of the experiment  $\approx 0.7^\circ$  allows a search window of  $1^\circ \times 1^\circ$  [24]. We begin with the “noise”. The event rate of the atmospheric  $\nu$ -background that will be detected in the search bin ( $\Delta\Omega_{1^\circ \times 1^\circ} \approx 3 \times 10^{-4}$  sr) is given by

$$\left. \frac{dN}{dt} \right|_{\text{background}} = A_{\text{eff}} \int dE J_{\nu+\bar{\nu}}(E) p(E) \Delta\Omega_{1^\circ \times 1^\circ}, \quad (6)$$

where  $A_{\text{eff}}$  is the effective area of the detector,  $J_{\nu+\bar{\nu}}(E)$  is the  $\nu_\mu + \bar{\nu}_\mu$  atmospheric flux in the direction of the Cygnus region (about  $40^\circ$  below the horizon) [25], and  $p(E) \approx 1.3 \times 10^{-6} (E/\text{TeV})^{0.8}$  denotes the probability (generic to ice/water detectors) that a  $\nu$  (or  $\bar{\nu}$ ) with energy  $E$  on a trajectory through the detector produces a signal [26]. For a year of running at IceCube and  $E_{\bar{\nu}}^{\text{min}} = 1$  TeV, from Eq. (6) one obtains a background of 1.5 events. Existing limits on the  $\gamma$ -ray flux from the

Cygnus region [27] provide an upper limit on neutrino fluxes generated via  $\pi^\pm$  decay at the source. This limit is below the atmospheric background in the region of interest. Poisson statistics then imply that a signal  $\geq 3.7$  events is significant at the 95% CL [28]. The number of  $\bar{\nu}$  showers in the signal, for energies above  $E_{\bar{\nu}}^{\text{min}}$ , is given by

$$\left. \frac{dN}{dt} \right|_{\text{signal}} = A_{\text{eff}} \int_{E_{\bar{\nu}}^{\text{min}}} dE_{\bar{\nu}} \frac{dF_{\bar{\nu}}}{dE_{\bar{\nu}}}(E_{\bar{\nu}}) p(E_{\bar{\nu}}). \quad (7)$$

For a year of running at IceCube, one expects 20 neutrino showers (all flavors) with energies  $\geq 1$  TeV, of which 4  $\bar{\nu}_\mu$  events will cluster within  $1^\circ$  of the source direction, comfortably above the stated CL. Neutrino flux at 1 TeV may also originate in the decay of 1 PeV neutrons from sources whose spectrum cuts off at that energy, and hence are not subject to normalization by the anisotropy. Thus our estimate may be regarded as very conservative.

IceCube is not sensitive to TeV neutrinos from the GC, as these are above the IceCube horizon, where atmospheric muons will dominate over any signal. However, other kilometer-scale neutrino detectors, such as those planned for the Mediterranean Sea, may see the GC flux.<sup>4</sup> Additionally, Southern Auger should see the cosmic ray excess in the direction of the GC [29] and Northern Auger should be sensitive to the Cygnus region.

We conclude that in a few years of observation, IceCube will attain  $5\sigma$  sensitivity for discovery of the  $\text{Fe} \rightarrow n \rightarrow \bar{\nu}_e \rightarrow \bar{\nu}_\mu$  cosmic beam, providing the “smoking ice” for the GP neutron hypothesis.

## Acknowledgments

We thank John Beacom, Jim Cronin, Concha Gonzalez-Garcia, Todor Stanev, and Alan Watson for valuable discussions. This work has been partially supported by NSF, DoE, NASA, and the Wisconsin Alumni Research Foundation.

- 
- [1] N. Hayashida *et al.* [AGASA Collaboration], *Astropart. Phys.* **10**, 303 (1999) [arXiv:astro-ph/9807045].
  - [2] M. Teshima *et al.*, *Proc. 27th International Cosmic Ray Conference*, (Copernicus Gesellschaft, 2001) p.341.

---

<sup>4</sup> The model depends on dilation of the neutron lifetime due to standard special relativity (SR). For neutrons from the GC, SR predicts stability at  $E_n \gtrsim 1$  EeV and decay at lower energies. Thus, if the model is validated, say through measurement of the predicted neutrino flux, then SR is validated to an unprecedented boost factor of  $\Gamma \approx 10^9$ , many orders of magnitude beyond present limits.

- [3] D. J. Bird *et al.* [HiRes Collaboration], *Astrophys. J.* **511**, 739 (1999) [arXiv:astro-ph/9806096].
- [4] J. A. Bellido, R. W. Clay, B. R. Dawson, and M. Johnston-Hollitt *Astropart. Phys.* **15**, 167 (2001) [arXiv:astro-ph/0009039].
- [5] F. A. Aharonian *et al.* [HEGRA Collaboration], *Astron. Astrophys.* **393**, L37 (2002) [arXiv:astro-ph/0207528].
- [6] Y. Butt *et al.*, *Astrophys. J.* **597**, 494 (2003) [arXiv:astro-ph/0302342].
- [7] J. Knodlseder, astro-ph/0007442.
- [8] M. Nagano *et al.*, *J. Phys. G* **18**, 423 (1992).
- [9] See *e.g.*, M. T. Dova, M. E. Mancenido, A. G. Mariazzi, T. P. Mc Cauley, and A. A. Watson, astro-ph/0305351.
- [10] S. P. Swordy *et al.*, *Astropart. Phys.* **18**, 129 (2002).
- [11] IceCube is the neutrino telescope under construction at the South Pole. <http://icecube.wisc.edu/>
- [12] The GZK or “cosmogenic” neutrinos are created as secondaries from the decay of charged pions produced in collisions between ultrahigh energy nucleons and the cosmic microwave background. K. Greisen, *Phys. Rev. Lett.* **16**, 748 (1966), G. T. Zatsepin and V. A. Kuzmin, *JETP Lett.* **4**, 78 (1966) [*Pisma Zh. Eksp. Teor. Fiz.* **4**, 114 (1966)]. For an update on GZK neutrinos, see *e.g.*, R. Engel, D. Seckel and T. Stanev, *Phys. Rev. D* **64**, 093010 (2001) [arXiv:astro-ph/0101216]; Z. Fodor, S. D. Katz, A. Ringwald and H. Tu, *JCAP* **0311**, 015 (2003) [arXiv:hep-ph/0309171].
- [13] G. L. Cassiday *et al.*, *Phys. Rev. Lett.* **62**, 383 (1989); M. Teshima *et al.*, *Phys. Rev. Lett.* **64**, 1628 (1990).
- [14] W. Bednarek, *Mon. Not. Roy. Astron. Soc.* **345**, 847 (2003) [arXiv:astro-ph/0307216].
- [15] P. Blasi, R. I. Epstein and A. V. Olinto, *Astrophys. J.* **533**, L123 (2000) [arXiv:astro-ph/9912240].
- [16] J. Arons, *Astrophys. J.* **589**, 871 (2003) [arXiv:astro-ph/0208444].
- [17] W. Bednarek and R. J. Protheroe, *Astropart. Phys.* **16**, 397 (2002) [arXiv:astro-ph/0103160].
- [18] C. D. Wilson, C. E. Walker and M. D. Thornley, arXiv:astro-ph/9701245.
- [19] M. M. Hanson, *Astrophys. J.* **597**, 957 (2003) [arXiv:astro-ph/0307540].
- [20] J. Knodlseder, M. Cervino, D. Schaerer, P. von Ballmoos and G. Meynet, arXiv:astro-ph/0104074.
- [21] This estimate makes use of secondary populations in high energy hadronic interactions as given in [J. Knapp, D. Heck and G. Schatz, *Nucl. Phys. Proc. Suppl.* **52B**, 136 (1997)], with a cut on  $\pi^\pm$  with energies  $> 2$  TeV.
- [22] S. N. Ahmed *et al.* [SNO Collaboration], nucl-ex/0309004.
- [23] J. Ahrens [AMANDA Collaboration], *Phys. Rev. Lett.* **92**, 071102 (2004) [arXiv:astro-ph/0309585].
- [24] J. Ahrens *et al.* [IceCube Collaboration], *Astropart. Phys.* **20**, 507 (2004) [astro-ph/0209556].
- [25] P. Lipari, *Astropart. Phys.* **1**, 195 (1993).
- [26] T. K. Gaisser, F. Halzen and T. Stanev, *Phys. Rept.* **258**, 173 (1995) [Erratum-ibid. **271**, 355 (1996)] [arXiv:hep-ph/9410384].
- [27] A. Borione *et al.* [CASA-MIA Collaboration], *Phys. Rev. D* **55**, 1714 (1997) [arXiv:astro-ph/9611117].
- [28] G. J. Feldman and R. D. Cousins, *Phys. Rev. D* **57**, 3873 (1998) [arXiv:physics/9711021]; N. Gehrels, *Astrophys. J.* **303**, 336 (1986).
- [29] R. W. Clay *et al.*, astro-ph/0308494.